Chemistry
A European
Journal

Chemistry Europe
European Chemical Societies Publishing

Accepted Article

Title: An NHC-stabilized phosphinidene for catalytic formylation: A DFT guided approach

Authors: Swadhin Kumar Mandal

To be cited as: *Chem. Eur. J.* 10.1002/chem.202101202

Link to VoR: https://doi.org/10.1002/chem.202101202

WILEY-VCH

10.1002/chem.202101202

WILEY-VCH

FULL PAPER

An NHC-stabilized Phosphinidene for Catalytic Formylation: A DFT Guided Approach

Sreejyothi P.[a], Kalishankar Bhattacharyya[b], Shiv Kumar[a], Pradip Kumar Hota[a], Ayan Datta[b]* and Swadhin K. Mandal[a]*

[a] Sreejyothi P, S.Kumar, Dr. P.K. Hota, Prof. S.K. Mandal
Department of Chemical Sciences
Indian Institute of Science Education and Research-Kolkata
Mohanpur-741246, India.
E-mail: swadhin.mandal@iiserkol.ac.in

[b] Dr. K. Bhattacharyya, Prof. A. Datta
Department of Spectroscopy
Indian Association for the Cultivation of Science
Jadavpur-700032, West Bengal (India)
E-mail: spad@iacs.res.in

Supporting information for this article is given via a link at the end of the document.((Please delete this text if not appropriate))

Abstract: *In recent years, applications of low-valent main group compounds in the field of catalysis are gaining momentum. NHC-stabilized phosphinidenes owing to the access of two lone pairs of electrons, have been found as excellent Lewis bases; however, they are yet to be used as catalysts. Herein, we report an NHC stabilized phosphinidene 1,3-dimethyl-2-(phenylphosphanylidene)-2,3-dihydro-1H-imidazole (**1**) for the activation of CO_2. A closer inspection of the CO_2 activation process by DFT calculations along with intrinsic bond orbital analysis unravels that phosphinidene is associated with phenylsilane through a non-covalent π-π interaction between two phenyl rings which activates the Si-H facilitating its transfer to the CO_2 molecule. Detailed DFT studies along with spectroscopic experiments were combined to understand the mechanism of CO_2 activation and its catalytic reductive functionalization leading to the formylation of a range of chemically inert primary amides under mild reaction conditions.*

Introduction

Phosphinidenes belong to neutral monovalent Group 15 analogues of carbenes possessing phosphorus in +1 oxidation state having access to two lone pairs of electrons.[1-4] Similar to the parent carbene ($:CH_2$), the parent phosphinidene exists in a triplet ground state with ΔE_{TS} = 22 kcal/mol.[5] Nevertheless, the ground state of phosphinidenes can be tuned into a stable singlet state by introducing appropriate substituents.[6] For example, in 1997, Arduengo and co-workers demonstrated that a singlet phosphinidene could be realized by N-heterocyclic carbene coordination to the phosphinidene moiety.[7] In following years, a number of singlet phosphinidenes have been synthetically accomplished by the groups of Robinson,[8] Bertrand,[9-10] Driess,[11] Tamm,[12-13] Roesky,[14-15] Grützmacher,[16] and others[17-18] stabilized by various carbenes. Recently, Bertrand and co-workers isolated a singlet phosphinidene at room temperature using a bulky N-heterocyclic phosphane.[19] The NHC stabilized phosphinidenes can best be presented by the two extreme canonical structures A and B (Scheme 1a). Form A refers to a carbon-phosphorus single bond with two lone pairs of electrons available on phosphorus whereas the form B represents a conventional phosphaalkene with a P-C double bond. Depending on the electronic property of carbene, the major valence bond form may switch from one extreme to another. In 2013, Bertrand and co-workers synthesized a series of NHC-phosphinidene adducts by introducing a range of electronically diverse NHCs and analysed them by ^{31}P NMR spectroscopic shifts.[9] It was observed that the NHC stabilized phosphinidenes displayed a high field chemical shift in ^{31}P NMR spectra in comparison to that observed for typical phosphalkenes (δ = 230-420 ppm),[20] which may be considered as an indication of a high electron density around phosphorus nucleus in these carbene stabilized phosphinidenes. On the other hand, the higher π acceptance property of NHC triggers the back donation from phosphorus to NHC, resulting in the relative downfield chemical shift in ^{31}P NMR spectroscopy.[9] Such an electronic influence suggests that the phosphinidenes can be made ambiphilic depending on the nature of stabilizing ligand.[21] The polarisation of P-C bond depends on the electronic properties of N-heterocyclic carbene as well as on the substituent on phosphorus center.[2] In 1997, Arduengo, Cowley and co-workers demonstrated that NHC stabilized phosphinidene ((IMes)PPh) [IMes = (1,3-dimesitylimidazolin-2-ylidene)] can form a bis(borane) adduct [{(IMes)PPh}$(BH_3)_2$] upon treatment with BH_3.^{THF}[22] (Scheme 1b). The formation of such bis borane adduct clearly suggests the availability of two lone pairs of electrons and strong nucleophilicity of phosphorus center. This result prompted many to consider NHC stabilized phosphinidene as a potential ligand for coordination to various metals.[12-13,17,23-28] Recently, IPr (1,3-bis(2,6-diisopropylphenyl)imidazol-2-ylidene) stabilized phosphinidene Au(I) complexes were used as catalysts in cycloisomerization of the 1,6-enynes to five- or six-membered 1,3-dienes (Scheme 1b).[13] Furthermore, NHC stabilized phosphinidenes were exploited for the activation of small

10.1002/chem.202101202

molecules. Ragogna *et al*. illustrated the efficiency of phosphinidenes in the ring-opening of THF in presence of a strong Lewis acid $B(C_6F_5)_3$ (Scheme 1b).[29] In 2013, Robinson *et al.* reported the activation of O_2 by an NHC stabilized phosphinidene dimer to form diphosphorus tetroxide (Scheme 1b).[30] However, beyond such small molecules' activation, the free phosphinidenes have not been explored in catalysis. In this regard, we strategized the possibility of utilizing phosphinidene as a metal-free catalyst. In 2017, Slootweg and Grützmacher reported an NHC stabilized phosphinidene adduct 1,3-dimethyl-2-(phenylphosphanylidene)-2,3-dihydro-1H-imidazole (**1**).

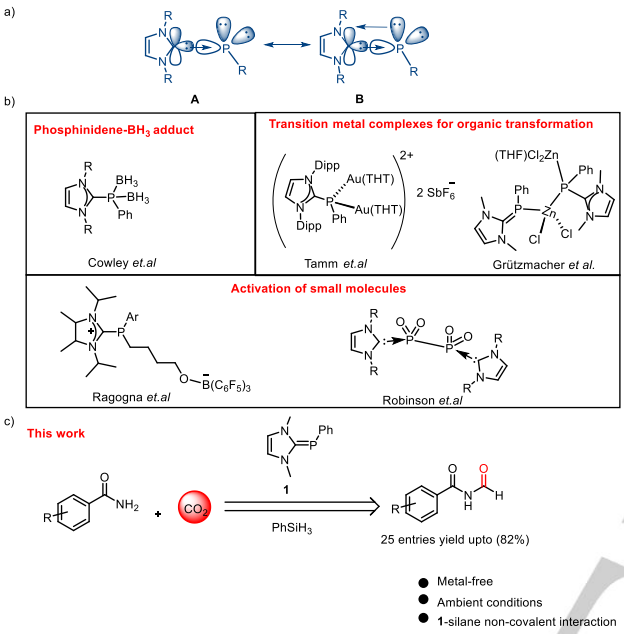

Scheme 1. a.Two extreme canonical structures of NHC stabilized phosphinidene. b. NHC-stabilized phosphinidenes used for various organic transformations. c. This work highlights the first catalytic application of phosphinidene resulting in activation of CO_2 to formylate a range of chemically inert primary amides under mild reaction conditions.

A preliminary DFT calculation on its bonding revealed the Wiberg bond index (WBI) of C(carbene)-P as 1.23 with C-P π bonded electron density mostly polarized towards the phosphorous centre (*vide infra*). This finding from DFT calculation along with its upfield ^{31}P NMR chemical shift, indicates a strong nucleophilic character of phosphorus in **1**. Thus encouraged, we attempted to explore this phosphinidene **1** towards the development of a metal-free catalyst. As a proof of concept, we have chosen catalytic formylation of primary amides, which proceeds through the activation of CO_2 by phosphinidene **1**. It is now established that CO_2 can be activated and functionalized by various nucleophilic metal-free catalysts such as N-bases, phosphanes, ionic liquids and various carbenes.[31] The area of metal-free catalytic activation of CO_2 is gaining tremendous attention due to its efficacy under mild reaction conditions as it avoids rare and heavy transition metals.[32-35] Recently, various low-valent main group compounds have been tested for their ability towards catalytic CO_2 activation with only limited success. For example, Inoue and co-workers demonstrated a neutral Al-Al double-bonded compound could fix CO_2, leading to its catalytic activation.[36] In this regard, low-valent phosphorus compounds also showed promise towards CO_2 activation, for example, Driess and co-workers demonstrated a silylene-stabilized zero-valent P_2 complex to activate CO_2 molecules in stoichiometric fashion.[37] However, low-valent phosphorus compounds such as phosphinidenes are yet to be realized as catalysts in CO_2 activation or in any organic transformation. Herein we report an NHC-stabilized phosphinidene **1** as a catalyst for CO_2 activation and formylation of chemically inert primary amides under ambient conditions. It may be noted that in literature, metal-free catalytic formylation of amines is quite well-studied.[38-41] Such formylation of amines using CO_2 has been accomplished with various low-valent metal-free main group compounds in recent time.[42-43] For example, reports by So and co-workers demonstrated the use of NHC-stabilized silylene[44] and N-phosphinoamidinato N-heterocyclic carbene-diborene[45] for catalytic formylation of amines using CO_2. On the contrary, the formylation of primary amides by metal-free catalyst has rarely been explored except in a recent report.[46] The catalytic formylation of primary amides using CO_2 is a challenging transformation as they are inert compared to amines toward such formylation. In this work, the NHC stabilized phosphinidene **1** was used as a catalyst for formylation of a range of primary amides at room temperature using CO_2 and silane under mild conditions. The nucleophilicity of **1** activates silane to incorporate CO_2 into Si-H bond leading to formyl transfer to the primary amides.

Results and Discussion

The NHC stabilized phosphinidene **1** was chosen for this study as the ^{31}P NMR data indicates that it has highly shielded phosphorus (δ = -57.2 ppm in CD_3CN) and it was prepared following the reported procedure.[28] At first, to get insight into the bonding scenario of the phosphinidene **1**, we have carried out density functional theory (DFT) calculations at the M06-2X/Def2-TZVP level of theory. Geometry optimization of **1** using the same level of theory suggests a closed-shell singlet ground state with a large ΔE_{ST} = 48.7 kcal/mol (Figure 1a).

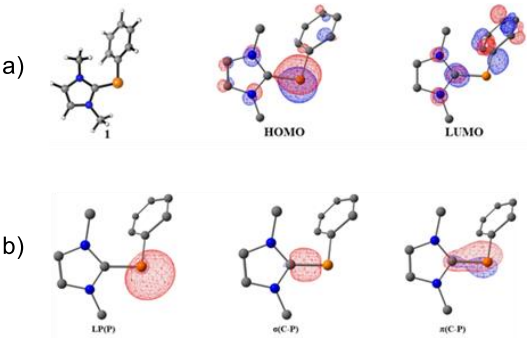

Figure 1. a) Optimized structure of **1** in singlet ground states at M06-2X/Def2-TZVP level of theory and the highest occupied and lowest unoccupied molecular orbitals (isosurface = 0.03 au). Hydrogen atoms are omitted for the sake of clarity. *Color code:* C, gray; N, blue; and P, orange. b) NBO orbitals of **1** (isosurface = 0.02 au) displaying electron density distribution of the lone pair of electrons on phosphorus, C-P σ bond and C-P π bond.

The bonding analysis reveals that the highest occupied molecular orbital (HOMO) of **1** corresponds to the π orbitals formed between the carbene carbon and phosphorus with a significant contribution coming from the phosphorus. On the other hand, LUMO has mostly π* orbital characteristics located on the carbene center of **1** (Figure 1a). The longer bond distance of $C_{carbene}$-P in **1** (1.78Å) in comparison to the classical phosphaalkenes ($C_{carbene}$-P ≈ 1.65-1.67Å) validates the phosphinidene character of **1**.[2] Further, Natural bond orbital (NBO) analyses demonstrate that $C_{carbene}$-P bond in **1** exhibits a partial double-bond character which is indicative from the Wiberg bond index (WBI) of $C_{carbene}$-P bond (1.23). Furthermore, NBO analysis reveals that electron density of the C-P σ bond in **1** is mainly polarized towards the carbene carbon ($C_{carbene}$(**1**): 67.7%), whereas C-P π bonded electron density is mostly polarized towards the phosphorous centre (70.1%, See Table S1). Such unsymmetrical π electronic distribution around the C-P bond of **1** supports its upfield chemical shift in ^{31}P NMR spectroscopy and is indicative of its nucleophilic nature. Next, we explored whether such nucleophilicity of **1** can be exploited in CO_2 activation. First, we performed a control reaction by mixing **1** (5 mol%) with phenylsilane (1 equiv) in acetonitrile in an argon-filled glovebox. Subsequently, it was taken to undergo two cycles of freeze pump and thaw which was then exposed to 1 atm CO_2 while warming up the frozen reaction mixture to room temperature. After 12 h, NMR spectroscopic analysis of the reaction mixture was performed and a peak at *δ* 8.4 ppm was observed in ^{1}H NMR spectrum, whereas ^{13}C NMR spectrum displayed a peak at *δ* 161.2 ppm in CD_3CN.[47] This observation suggests activation of CO_2 by **1** in presence of silane resulting in the formation of phenylsilane formate (**5**) in which CO_2 got inserted into the Si-H bond of phenylsilane. Our efforts to isolate the phenylsilane formate (**5**) failed, as it decomposed during isolation. However, this initial finding prompted us to take up further detailed investigation to understand such CO_2 activation in presence of **1** and phenylsilane. DFT studies proposed the formation of a π- π stacked phosphinidene-phenylsilane adduct **1a** (Figure 2a) with favourable binding energy -8.3 kcal/mol, while such non-negligible interaction weakens the Si-H bond (~1.49 Å) as compared to the Si-H bond length calculated in free silane (1.45 Å). In order to understand such interaction between **1** and phenylsilane, DFT calculation was undertaken and it revealed that upon interaction of phenylsilane with **1**, they associate as **1a** through a π-stacking interaction between two adjacent phenyl rings with a separation of 3.69 Å. Optimized structure of 1-silane adduct (**1a**) is displayed in Figure 2a where P and Si are separated by a distance of 3.63 Aº indicating a very weak interaction. Dispersion interaction density plot of the **1a** shows that non-covalent π-stacking interactions are mainly arising from the rather strong London dispersion forces (Figure 2b). stabilizing the π-stacked complex by -8.3 kcal/mol. Note that the M06-2X DFT functional has been shown to be successful in describing middle-range dispersion interactions like π-stacking.[48] We further evaluated the non-covalent interactions using open source NCI code.[49-50] As shown in Figure 2c, non-covalent electron density (shown in green) between the phenyl rings of the adduct is attributed to the strong π-π interactions between them. The large separation between P and Si centers (3.63 Å) in **1a** supports almost negligible direct interaction between them; however, on addition of CO_2, the P and Si distance reduce to 2.56 Å (**TS1**). Further, it significantly weakens the Si-H bond (~1.72 Å) and favours the hydride transfer to CO_2 with a free-energy of activation of 15.8 kcal/mol through the **TS1** as shown in Figure 2d. Such Si-H activation mode for CO_2 reduction also was reported in the literature previously.[51] Further, the WBI calculations reveal that C-P bond of phosphinidene attains a significantly reduced value of 0.99 in **TS1** from its original value 1.23 calculated for free **1,** which strongly supports the flow of π- electron density from P center during activation of CO_2 molecule (*vide infra*).

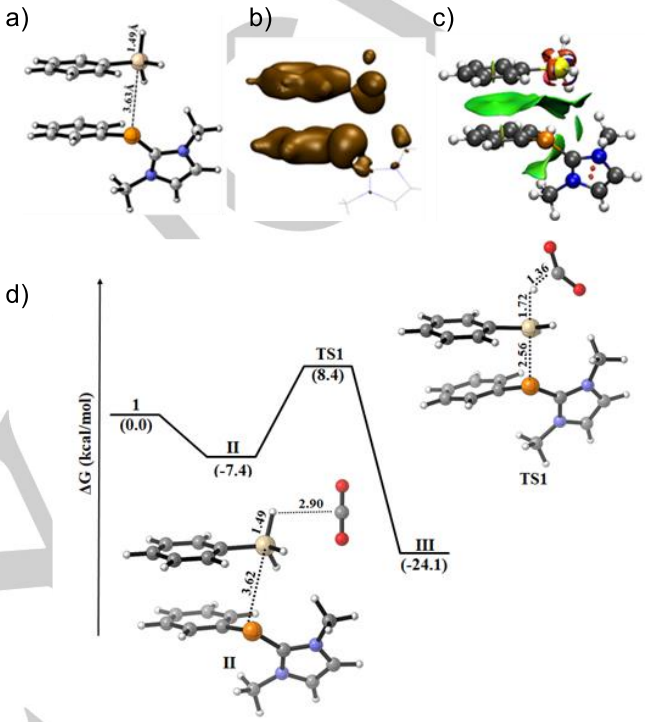

Figure 2. a) Optimized structure of phosphinidene-silane adduct **1a**. b) Dispersion interaction density plot of **1a**. c) Non-covalent interaction plot (NCI) of the **1**-phenylsilane adduct showing the non-covalent electron density. d) The relative Gibbs free energies for 298 K (in kcal/mol) at M06-2X/6-311++G(d,p)(SMD:acetonitrile) level of theory. Optimized structures of selected intermediate and transition state structures are also represented. Distances are in Å.

In order to check the stability of catalyst during the activation of CO_2, we have performed a low temperature ^{31}P{^{1}H} NMR analysis of the catalytic reaction mixture in presence of CO_2. In such experiment, an equimolar amount of **1** and phenylsilane were loaded in a J Young NMR tube in CD_3CN, subjected to two cycles of freeze, pump and thaw, and exposed to CO_2 at low temperature (~-40 °C). ^{31}P{^{1}H} NMR analysis of the reaction mixture, in a precooled NMR probe at -35°C confirmed the presence of **1** in the reaction medium (see SI Fig S45). For deeper understanding of CO_2 activation by **1a**, we have carried out the intrinsic bond orbital (IBO) analysis scheme developed by Knizia et al.[52] This procedure is extensively applied to understand the bond breaking/bond making process along the reaction coordinate.[53-54] Here, the evolution of IBO along the intrinsic reaction coordinates of the transition states as shown in Figure 3. have been assessed to analyse the relevant electron density flow from **1** to phenylsilane during the CO_2 activation. As shown in Figure 3, three IBOs corresponding to the *π*(CNHC-P), σ (P-Si), and σ (Si-H) bond have revealed significant charge flux along the intrinsic

10.1002/chem.202101202

reaction coordinate (IRC). Figure 3. demonstrates the IBO (purple lobe) of the C-P bond of **1** being transformed into the P-Si bond while IBO (light blue lobe) evolves from a Si-H bond in silane to a C-H bond on the CO_2. Upon closer inspection to the orbital distribution along the reaction coordinate, it reveals that π bond of the C-P in **1** is transforming into the

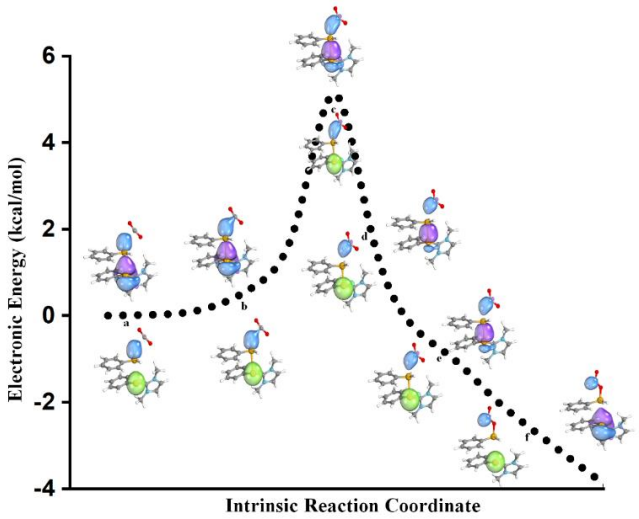

Figure 3. Intrinsic bond orbital analysis of the selected geometries along Intrinsic reaction coordinate (IRC) of transition-state during CO_2 activation by **1**. Intrinsic bond orbital (IBO) transformations along the P-Si bond are shown in purple lobe and dissociation of Si-H towards electrophilic C centers of CO_2 are shown in blue. Transformations of Si-H to C-H bonds are shown as blue lobe and intrinsic bond orbital (green lobe) corresponding to lone pair of electrons on phosphorus center remains unaltered along the reaction coordinates. a, b, c, d, e, and f correspond to the selected geometries from the IRC.

σ-bond between the P-Si bond. However, IBO (green lobe) corresponding to the lone-pair of electrons on the phosphorus atom in **1** remains preserved along the reaction coordinates as shown in Figure 3. Since electronic redistribution occurs from the π bond of the C-P towards the P-Si bond during the CO_2 activation, therefore **1** acts as a strong nucleophile to complete the CO_2 activation via silane activation through the formation of **1**-silane adduct **1a**. Calculated WBI ~1.20 of C-P bond in **1a** also explains the electronic redistribution for the activation mechanism of CO_2 as it reduced significantly to 0.99 in the TS1 (Figure 2d, *vide supra*). These findings on CO_2 activation by the NHC stabilized phosphinidene **1** in the presence of a silane prompted us towards the development of a catalytic process. We have chosen the formylation of primary amides by CO_2 as a model transformation since amide formylation has been considered extremely challenging because of their inertness towards chemical functionalization. Until 2018, the catalytic formylation of amide was not known and till date only one study has been reported for catalytic formylation of primary amides under metal-free conditions.[46] N-formyl amides have widespread applications in pharmaceutical industry in which they represent the synthetic intermediates of many natural products.[55] Further they belong to important class of reagents in several reactions as well as act as amino protecting groups in peptide synthesis.[56] In our optimization study, 2-methyl benzamide (**2a**) was used as a standard substrate. It was found that 10 mol% **1** can perform catalytic formylation of primary amides in 24 h using CO_2 and $PhSiH_3$ under ambient temperature with 37% NMR conversion (Table 1, entry 1). Under such conditions, various solvents such as acetonitrile, toluene, chlorobenzene, dioxane, hexane were screened (Table 1, entries 2-6) and it was observed that acetonitrile delivers the best conversion (75%). It may be noted that polar solvents such as THF, acetonitrile and dioxane provided better reactivity as compared to the other non-polar solvents such as hexane and toluene. Such an observation may be accounted for the better solubility of CO_2 in polar solvents as also reported in a recent study.[57] Next, we screened other silanes such as Et_3SiH, Ph_2SiH_2 and PMHS (Table 1, entries 7-9), however, the reaction did not yield the desired product. From this optimization study, it may be concluded that under 1 atm CO_2, 10 mol% catalyst delivered the best yield of formylated product (Table 1, entry 3). With this optimized condition in hand, we explored various amide substrates for reductive formylation to establish efficacy of **1** as a catalyst. The formylation reaction with benzamide resulted in 75% isolated yield upon purification using silica gel chromatography (Table 3, **3b**). Electron donating methyl-substituted benzamides

Table 1. Optimization of reaction conditions for formylation of primary amides using **1** as a catalyst.

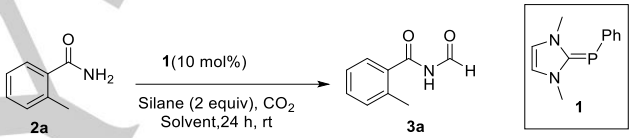

Sl No.	Silane	Solvent	Conversion (%)
1	$PhSiH_3$	THF	37
2	$PhSiH_3$	Toluene	NR
3	**$PhSiH_3$**	**Acetonitrile**	**75**
4	$PhSiH_3$	Chlorobenzene	12
5	$PhSiH_3$	Hexane	NR
6	$PhSiH_3$	Dioxane	20
7	Et_3SiH	Acetonitrile	NR
8	Ph_2SiH_2	Acetonitrile	NR
9	PMHS	Acetonitrile	NR

[a] **Reaction conditions**: Amide (0.3 mmol), silane (0.6 mmol), **1** (0.03 mmol, 10 mol%), and solvent (1 mL), NR stands for "No Reaction"

delivered corresponding formylated products **3a** (68%), **3d** (74%), **3e** (61%) in good to very good isolated yields whereas electron-withdrawing substrates afforded **3l** (56%), **3n** (57%) in moderate yield. However, substrates possessing both electron-donating and withdrawing substituents delivered 56% yield (**3j**). In presence of chloride substitution, primary amides displayed low reactivity towards formylation resulting in **3r** (43%), **3m** (40%) and

10.1002/chem.202101202

3q (53%). In addition, the catalyst was efficient in performing the formylation of heteroatom containing amides in good to moderate yield of **3i** (71%) and **3s** (49%). Substrates bearing the nitro group afforded **3p** in 45% and **3o** in 43% yield. Biphenylamide displayed low reactivity yielding 33% (**3t**) whereas cinnamamide tolerated the reaction conditions resulting in a yield of 48% (**3g**). However, the reaction proceeded smoothly in presence of 2-/3-/4-methoxy substituted benzamide in 72%, 76%, 82% (**3c**, **3k**, **3h**), respectively while 2-ethoxy substituted benzamide led to 69% (**3f**) yield. We were delighted to observe that **1** acts as an effective catalyst in promoting the formylation of various aliphatic primary amides (linear and cyclic) with an NMR conversion ranging from 27-77% (**3u**-**3y**).

Table 2. Formylation of primary amides using the NHC stabilized phosphinidene **1** as a catalyst.

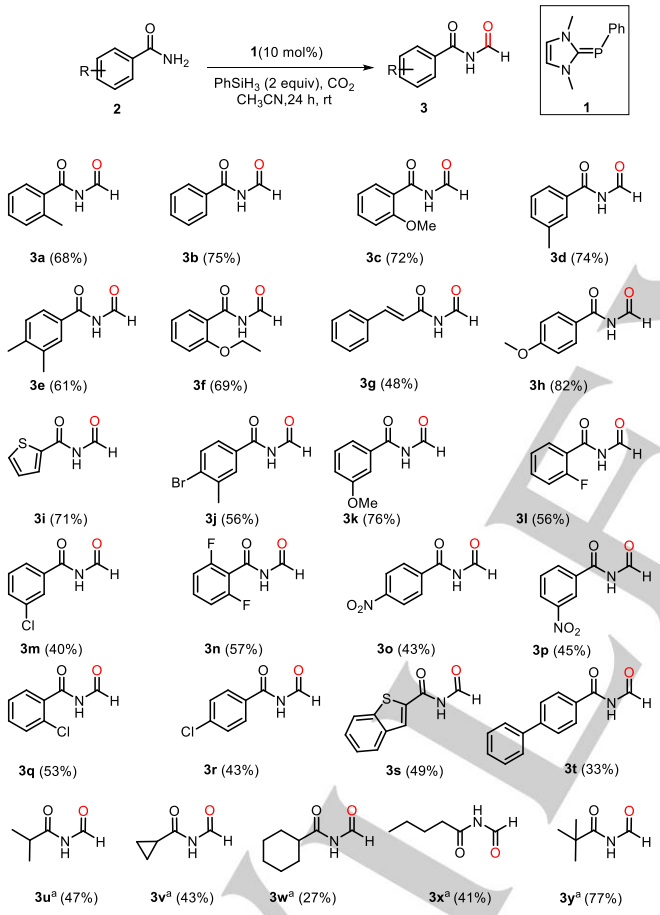

Reaction conditions. Amide (0.3 mmol), $PhSiH_3$ (0.6 mmol), **1** (0.03 mmol, 10 mol%), and ACN (1 mL), Isolated yield in the parenthesis. [a] NMR conversion using hexamethylbenzene as an internal standard.

This result establishes that NHC stabilized phosphinidene **1** can act as an efficient catalyst for formylation of a range of primary amides using CO_2 under mild conditions. Based on the above findings from control experiments and DFT calculations, a plausible catalytic cycle is proposed in Scheme 2.

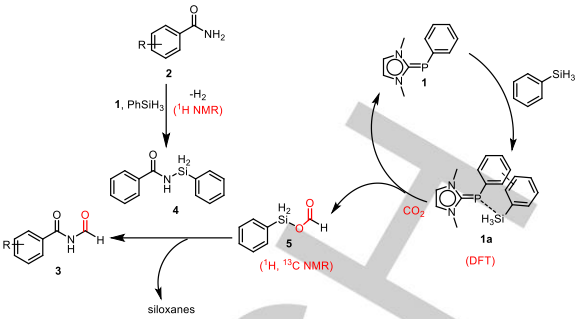

Scheme 2 Plausible mechanistic cycle for formylation of primary amides using NHC-stabilized phosphinidene **1.**

At first, **1** interacts with $PhSiH_3$ through π-π interaction between two adjacent phenyl rings which initiates activation of the Si-H bond (Figure 2a). Upon interaction of the CO_2 molecule with such π-π stacked adduct **1a**, the C-P π bonded electron density flows to further activate the Si-H bond resulting in its facile transfer to the CO_2 molecule (Figures 2d and 3), leading to the formation of phenylsilyl formate which has been characterized by NMR spectroscopy.[50] It may be noted that the activation of CO_2 proceeds by a concerted pathway as depicted in Figure 3, and this step is exergonic by -16.7 kcal/mol and therefore, it drives the formylation reaction (Figure 4).

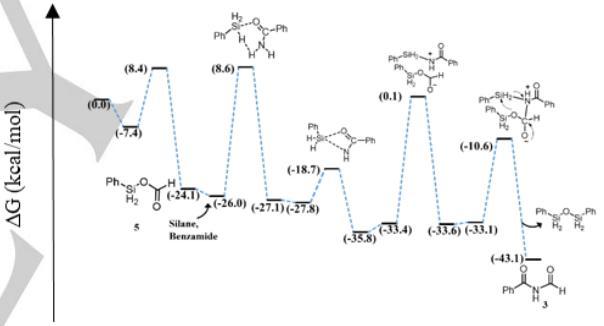

Figure. 4 Computed Gibbs free energy profile at 298 K using NHC stabilized phosphinidene catalyst for formylation of benzamide using CO_2.

Simultaneously in presence of **1,** phenylsilane undergoes dehydrogenation reaction with amide to form N-silylated amide (**4**) on liberation of H_2 molecule which was identified by ^1H NMR spectroscopic analysis (δ 4.58 ppm in CD_3CN)[58] as well as GC-MS analysis (Figure S50, SI) in a control reaction. Similar activation of primary amides upon liberation of hydrogen molecule by 9-BBN via N-borylation of primary amide has been reported in recent literature.[59] Upon the formation of the N-silylated amide, it reacts with the phenylsilyl formate. Subsequently, the formyl transfer takes place from **5** to **4** and the reaction proceeds through various transition states as depicted in Figure 4 leading to the formation of desired product **3** along with siloxanes as the by-product, also reported previously.[44] Furthermore, in a control experiment, triphenylsiloxane Ph_3Si-O-$SiPh_3$ was identified as the by-product by ^1H and ^{29}Si NMR spectroscopy when Ph_3SiH was used as the reducing agent.[46]

Conclusion

In conclusion, an NHC stabilized phosphinidene **1** was used as the first metal-free catalyst in any organic transformation. Catalyst **1** effectively performed the formylation of a range of primary amides using CO_2 as a reagent under ambient temperature. The CO_2 activation is facilitated by a proposed weakly bound phosphinidene-silane intermediate. Detailed DFT studies and control experiments helped us to understand the underlying mechanism involved in this transformation. London dispersion force between the π-stacked aromatic rings along with the nucleophilicity of **1** plays a crucial role in structural reorganization of the catalyst. This result paves the way towards designing strategy to use phosphinidenes as catalysts towards various organic transformations.

Experimental Section

Materials and Methods

All reactions were performed in oven dried glassware (130 ^oC) under dry and oxygen free atmosphere (Argon) using standard Schlenk line technique or inside Ar filled MBraun glovebox which is maintained at <0.1 ppm level of O_2 and H_2O. The solvents used for the reaction were dried using Na/benzophenone mixture or CaH_2 before use. All chemicals were purchased from Sigma-Aldrich, Alfa Aesar, Merck, or Spectrochem and used as received. **1** was prepared following the reported procedure.[28] Thin-layer chromatography (TLC) was performed on a Merck 60 F254 silica gel plate (0.25 mm thickness). Column chromatography was performed on a Merck 60 silica gel (100−200 mesh).GC-MS analysis was carried out using Clarus 590 GC-MS instrument (Perkin Elmer). The ^1H,^{13}C,^{31}P and ^{29}Si NMR spectra were recorded on JEOL ECS 400 MHz spectrometer and on Bruker Avance III 500 MHz spectrometer with residual proton resonances (for $CDCl_3$:^1H at δ = 7.26, $^{13}C\{^1H\}$ at δ = 77.16, CD_3CN: ^1H at δ = 1.94, $^{13}C\{^1H\}$ at δ = 1.32, for DMSO: ^1H at δ = 2.5, $^{13}C\{^1H\}$ at δ = 39.5. Carbon dioxide was purchased from Praxair in a 5.5 purity gas cylinder with 99.995% purity.

Computational Methods

All geometry optimization, singlet point calculations, vibrational frequency and reaction free energies were carried out using density functional theory through the Gaussian 16 suite of programs.[60] To determine spin multiplicity of ground state of the complexes, both restricted and unrestricted calculations were performed in the gas phase using hybrid meta-GGA M06-2X functional[61] in conjunction with Def2-TZVP basis set of theory using ORCA.[62] Natural bond orbital analysis (NBO) and Wiberg bond indices (WBI) were performed at the M06-2X/Def2-TZVP level of theory using the NBO6 version.[63] For main group element, M06-2X is highly recommended for the thermochemical calculations, henceforth M06-2X/6-31+G(d) level of theory was conducted to describe the reaction energy of reductive functionalization of CO_2. Harmonic vibrational frequencies were calculated at same level of theory to ensure the absence of saddle point of intermediate geometries and only one imaginary frequency in transition state structures. IRC calculation was further performed to confirm that the TS structure connected with reactants and products. To account the solvation energies in acetonitrile, self-consistent reaction field (SCRF) approach using SMD continuum solvation model has been utilized.[64] Furthermore, to improve the accuracy of the reaction energies obtained from the M06-2X/6-31+G(d,p) level of theory, single-point calculations were carried out using triple-ζ valance shell with additional diffuse and polarization basis set (6-311++G(d,p)) on the top of the optimized geometries. All the free energies are obtained from the M06-2X/6-311++G(d,p)(SMD)//M06-2X/6-31+G(d,p) level of theory at 298 K. To investigate the intrinsic bond orbitals (IBO), single point calculations were recomputed along the each points of IRCs using ORCA, to generate the IBO plots using the IboView program with iboexp=2.[65]

General procedure for the formylation of primary amides.

Under an argon atmosphere, a 25 mL Schlenk tube equipped with a stir bar and a J. Young valve was charged with amide (0.3 mmol), **1** (10 mol%), phenylsilane (0.6 mmol) and acetonitrile (1 mL). For substrate having Br or Cl or NO_2 substituent, 100 µL DMSO was added for the solubility. The mixture was degassed by two successive freeze-pump-thaw cycles and was exposed with carbon dioxide in the frozen state. The reaction mixture was allowed slowly to warm to room temperature and stirred for 24 h. Next, the solvent was evaporated under reduced pressure and the product was purified by column chromatography on silica gel (Merck, 100-200 mesh). The N-formyl amide was collected as an analytically pure solid using hexane-ethyl acetate mixture as the eluent. The corresponding formamide was identified by ^1H and ^{13}C NMR spectroscopy in $CDCl_3$ or DMSO-d_6 or $CDCl_3$ and DMSO-d_6 mixture.

Acknowledgements

We acknowledge financial support from the MHRD-STARS project, (STARS/APR2019/CS/473/FS). S.P thanks DST Inspire for research fellowship. A.D thanks SERB project, CRG/2020/000301 Intrinsic bond orbital analysis for support. K.B acknowledges IACS for a research fellowship. We thank Dr. Rangeet Bhattacharya for the help in VT NMR experiments.

Keywords: Phosphinidene • DFT • Intrinsic bond orbital analysis • CO_2 activation • Amide formylation

[1] F. Mathey, *Angew. Chem., Int. Ed.* **1987**, *26*, 275-286; *Angew. Chem*. **1987**, *99*, 285-296.
[2] T. Krachko, J. C. Slootweg, *Eur. J. Inorg. Chem.* **2018**, 2734-2754.
[3] A. Doddi, M. Peters, M. Tamm, *Chem. Rev*. **2019**, *119*, 6994-7112.
[4] K. Lammertsma, *Top. Curr. Chem*. **2003**, *229*, 95-119.
[5] F. Zittel, W. C. Lineberger, *J. Chem. Phys*. **1976**, *65*, 1236-1243.
[6] T. Nguyen, A. Van Keer, L. G. Vanquickenborne*, J. Org. Chem*. **1996**, *61*, 7077-7084.
[7] A. J. Arduengo III, H. V. R. Dias, J. C. Calabrese, *Chem. Lett*. **1997**, *26*, 143-144.
[8] Y. Wang, Y. Xie, M.Y. Abraham, R.J. Gilliard Jr., P. Wei, H.F. Schaefer III, P.v.R. Schleyer,G.H. Robinson, *Organometallics* **2010**, *29*, 4778-4780.
[9] O. Back, M. Henry-Ellinger, C.D. Martin, D. Martin, G. Bertrand, *Angew. Chem. Int. Ed.* **2013**, *52***,** 2939–2943; *Angew.Chem*. **2013**,*125*, 3011–3015.
[10] L. Liu, D. A. Ruiz, F. Dahcheh, G. Bertrand, *Chem. Commun*. **2015**, *51*, 12732–12735.
[11] K. Hansen, T. Szilvási, B. Blom, S. Inoue, J. Epping, M. Driess, *J. Am. Chem. Soc*. **2013**, *135*, 11795-11798.
[12] A. Doddi, D. Bockfeld, T. Bannenberg, P. G. Jones, M. Tamm, *Angew. Chem. Int. Ed.* **2014**, *53*, 13568-13572; *Angew.Chem*. **2014**, *126*,13786-13790.
[13] A. Doddi, D. Bockfeld, A. Nasr, T. Bannenberg, P. G. Jones, M. Tamm, *Chem. Eur. J.* **2015**, *21*, 16178–16189.
[14] S. Roy, K. C. Mondal, S. Kundu, B. Li, C. J. Schürmann, S. Dutta, D. Koley, R. Herbst-Irmer, D. Stalke, H. W. Roesky, *Chem. Eur. J.* **2017**, *23*, 12153–12157.
[15] S. Kundu, S. Sinhababu, A. V. Luebben, T. Mondal, D. Koley, B. Dittrich, H. W. Roesky, *J. Am. Chem. Soc*. **2018**, *140*, 151–154.
[16] A.M. Tondreau, Z. Benkö, J.R. Harmer**,** H. Grützmacher, *Chem. Sci*. **2014**, *5***,** 1545–1554.

[17] V. A. K. Adiraju, M. Yousufuddin, H. V. R. Dias, *Dalton Trans*. **2015**, *44*, 4449-4454.
[18] H. Schneider, D. Schmidt, U. Radius, *Chem. Commun.* **2015**, *51*, 10138-10141.
[19] L. Liu, D. A. Ruiz, D. Munz, G. Bertrand, *Chem* **2016**, *1*, 147-153.
[20] M. Regitz and O. J. Scherer, *Multiple Bonds and Low Coordination Phosphorus Chemistry*, Georg Thieme, Stuttgart and NewYork, **1990,** p.157.
[21] M. M. Hansmann, R. Jazzar, G. Bertrand, *J. Am. Chem. Soc.* **2016**, *138*, 8356-8359.
[22] A. J. Arduengo III, C. J. Carmalt, J. A. C. Clyburne, A. H. Cowley, R. Pyati, *Chem. Commun.* **1997**, 981–982.
[23] T. G. Larocque, G. G. Lavoie, *New J. Chem*. **2014**, *38*, 499-502.
[24] L. Liu, D. A. Ruiz, F. Dahcheh, G. Bertrand, *Chem. Commun*. **2015**, *51*,12732–12735.
[25] D. Bockfeld, A. Doddi, P. G. Jones, M. Tamm, *Eur. J. Inorg. Chem*. **2016**, 3704–3712.
[26] M. Klein, G. Schnakenburg, A. Espinosa Ferao, N. Tokitoh, R. Streubel, *Eur.J. Inorg. Chem*. **2016**, 685–690.
[27] M. Peters, A. Doddi, T. Bannenberg, M. Freytag, P. G. Jones, M. Tamm, *Inorg. Chem*. **2017**, *56*, 10785–10793.
[28] T. Krachko, M. Bispinghoff, A. M. Tondreau, D. Stein, M. Baker, A. W. Ehlers, J. C. Slootweg, H. Grützmacher, *Angew. Chem. Int. Ed*. **2017**, *56*, 7948–7951; *Angew. Chem*. **2017**, *129*, 8056-8059.
[29] C. M. E. Graham, C. R. P. Millet, A. N. Price, J. Valijus, M. J. Cowley, H. M. Tuononen, P. J. Ragogna, *Chem. Eur. J.* **2018**, *24*, 672–680.
[30] Y. Wang, Y. Xie, P. Wei, H. F. Schaefer III, P. V. R. Schleyer, G. H. Robinson, J. *Am. Chem. Soc*. **2013**, *135*, 19139-19142.
[31] P. Sreejyothi, S. K. Mandal, *Chem. Sci.* **2020**, *11*, 10571–10593.
[32] F.-G. Fontaine, M.-A. Courtemanche, M.-A. Légaŕe, *Chem. Eur.J.* **2014**, *20*, 2990-2996.
[33] G. Fiorani, W. Guo, A. W. Kleij, *Green Chem.* **2015**, *17*, 1375-1389.
[34] A. Tlili, E. Blondiaux, X. Frogneux, T. Cantat, *Green Chem.* **2015**, *17*, 157-168.
[35] M. Hulla, P. J. Dyson, *Angew. Chem. Int. Ed*. **2020**, *59*, 1002-1017; *Angew. Chem*. **2020**, *132*, 1014-1029.
[36] P. Bag, C. Weetman, S. Inoue, *Angew. Chem. Int. Ed.* **2018**, *57*, 14394-14413; *Angew. Chem*. **2018**, *130*, 14594-14613.
[37] Y. Wang, T.Szilvasi, S. Yao, M. Driess, *Nat. Chem*. **2020**, *12*, 801−807.
[38] C. Das Neves Gomes, O. Jacquet, C. Villiers, P. Thuéry, M. Ephritikhine, T. Cantat, *Angew. Chem. Int. Ed*. **2012**, *51*, 187-190; *Angew. Chem*. **2012**, *124*, 191-194.
[39] O. Jacquet, C. Das Neves Gomes, M. Ephritikhine, T. Cantat, *J. Am. Chem. Soc.* **2012**, *134*, 2934-2937.
[40] L.-D. Hao, Y.-F. Zhao, B. Yu, Z.-Z. Yang, H.-Y. Zhang, B.-X. Han, X. Gao, Z.-M. Liu, *ACS Catal.* **2015**, *5*, 4989-4993.
[41] M. Hulla, F. D. Bobbink, S. Das, P. J. Dyson, *ChemCatChem* **2016**, *8*, 3338-3342.
[42] C. C. Chong, R. Kinjo, *Angew. Chem. Int. Ed.* **2015**, *54*, 12116-12120; *Angew. Chem.* **2015**, *127*, 12284-12288.
[43] D. Sarkar, C. Weetman, C. Dutta, E. Schubert, C. Jandl, D. Koley, S. Inoue, *J. Am. Chem. Soc.* **2020**, *142*, 15403-15411.
[44] B.-X. Leong, Y.-C. Teo, C. Condamines, M.-C. Yang, M.-D. Su, C.-W. So, *ACS Catal.* **2020**, *10*, 14824-14833.
[45] J. Fan, J.-Q. Mah, M.-C. Yang, M.-D. Su, C.-W. So, *J. Am. Chem. Soc*. **2021**, *143*, 4993-5002.
[46] P. K. Hota, S. C. Sau, S. K. Mandal, *ACS Catal*. **2018**, *8*, 11999-12003.
[47] A. Gopakumar, L. Lombardo, Z. Fei, S. Shyshkanov, D. Vasilyev, A. Chidambaram, K. Stylianou, A. Züttel and P. J. Dyson, *J. CO_2 Util*. **2020**, *41*, 101240.
[48] A. Nijamudheen, D. Jose, A. Shine, A. Datta, *J. Phys. Chem. Lett.* **2012**, *3*, 1493-1496.
[49] J. Contreras-García, E. R. Johnson, S. Keinan, R. Chaudret, J.-P. Piquemal, D. N. Beratan, W. Yang, *J. Chem. Theory Comput.* **2011**, *7*, 625–632.
[50] E. R. Johnson, S. Keinan, P. Mori-Sánchez, J. Contreras-García, A. J. Cohen, W. Yangm, *J. Am. Chem. Soc.* **2010**, *132*, 6498-6506.
[51] Q. H. Zhou and Y. X. Li, *J. Am. Chem. Soc.* **2015**, *137*, 10182-10189.
[52] G. Knizia, *J. Chem. Theory Comput.* **2013**, *9*, 4834-4843.
[53] W.-M. Ching, A. Zhou, J. E. M. N. Klein, R. Fan, G. Knizia, C. J. Cramer, Y. Guo and L. Que, Jr., *Inorg. Chem.* **2017**, *56* , 11129-11140 .
[54] M. Mandal, C. E. Elwell, C. J. Bouchey, T. J. Zerk, W. B. Tolman, C. J. Cramer, *J. Am. Chem. Soc*. **2019**, *141*, 17236-17244.
[55] J. E. Mathieson, J. J. Crawford, M. Schmidtmann, R. Marquez, *Org. Biomol. Chem*. **2009**, *7*, 2170–2175.
[56] P. V. S. Ramya, S. Angapelly, B. N. Babu, C. S. Digwal, A. Nagarsenkar, S. Gannoju, B. Prasanth, M. Arifuddin, K. Kanneboina, K. Rangan, A. Kamal, *Asian J. Org. Chem*. **2017**, *6*, 1008-1013.
[57] A. Cerveri, R. Giovanelli, D. Sella, R. Pedrazzani, M. Monari, O. N. Faza, C. S. López, M. Bandini, *Chem. Eur. J.* **2021**, DOI: 10.1002/chem.202101082.
[58] G. R. Fulmer, A. J. M. Miller, N. H. Sherden, H. E. Gottl 10.1002/chem.202101082ieb, A. Nudelman, B. M. Stoltz, J. E. Bercaw, K. I. Goldberg, *Organometallics* **2010**, *29*, 2176-2179.
[59] M. Bhunia, S. R. Sahoo, A. Das, J. Ahmed, P. Sreejyothi, S. K. Mandal, *Chem. Sci.* **2020**, *11*, 1848-1854.
[60] M. J. Frisch, G. W. Trucks, H. B. Schlegel, G. E. Scuseria, M. A. Robb, J. R. Cheeseman, G. Scalmani, V. Barone, G. A. Petersson, H. Nakatsuji, X. Li, M. Caricato, A. V. Marenich, J. Bloino, B. G. Janesko, R. Gomperts, B. Mennucci, H. P. Hratchian, J. V. Ortiz, A. F. Izmaylov, J. L. Sonnenberg, D. Williams-Young, F. Ding, F. Lipparini, F. Egidi, J. Goings, B. Peng, A. Petrone, T. Henderson, D. Ranasinghe, V. G. Zakrzewski, J. Gao, N. Rega, G. Zheng, W. Liang, M. Hada, M. Ehara, K. Toyota, R. Fukuda, J. Hasegawa, M. Ishida, T. Nakajima, Y. Honda, O. Kitao, H. Nakai, T. Vreven, K. Throssell, J. A. Montgomery, Jr., J. E. Peralta, F. Ogliaro, M. J. Bearpark, J. J. Heyd, E. N. Brothers, K. N. Kudin, V. N. Staroverov, T. A. Keith, R. Kobayashi, J. Normand, K. Raghavachari, A. P. Rendell, J. C. Burant, S. S. Iyengar, J. Tomasi, M. Cossi, J. M. Millam, M. Klene, C. Adamo, R. Cammi, J. W. Ochterski, R. L. Martin, K. Morokuma, O. Farkas, J. B. Foresman, D. J. Fox, *Gaussian 16, Revision A.03, Gaussian, Inc.*, Wallingford CT, **2016**.
[61] Y. Zhao,D. G. Truhlar, *Theor. Chem. Acc.* **2008**, *120*, 215-241.
[62] F. Neese, The ORCA program system. *Wiley Interdiscip. Rev. Comput. Mol. Sci.* **2012**, *2*, 73-78.
[63] F. Weinhold, C. R. Landis, Cambridge University Press: Cambridge, UK, **2005**
[64] A. V. Marenich, C. J. Cramer, D. G Truhlar, *J. Phys. Chem. B*. **2009**, *113*, 6378−6396.
[65] E. R. Hoffman, Magn. Reson. *Chem*. **2006**, *44*, 606-616.

10.1002/chem.202101202

Entry for the Table of Contents

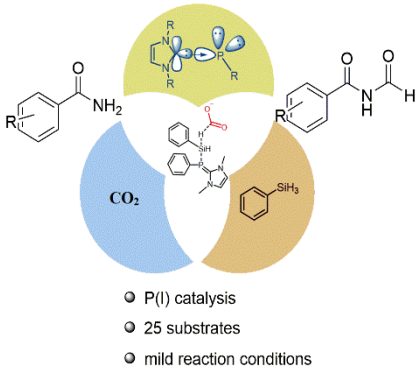

This work highlights introduction of a low-valent phosphorus compund in the arena of catalysis in which N-heterocyclic carbene stabilized phosphinidene (**1**) was utlized for the activation of CO_2. The DFT calculations unravel that nucleophilicilty of the phosphorus center and a non-colvant π-π interaction between the phenyl rings of phenylsilane and the catalyst syngersticaly drives the formylation of primary amides by CO_2 under mild conditions.